

COMPUTATIONAL STUDY OF TURBINE BLADE FILM COOLING  
PERFORMANCE USING ANISOTROPIC TURBULENCE MODELS

CHANDRAN SUNDARAJ

A thesis submitted in fulfilment of the  
requirements for the award of the degree of  
Master of Engineering (Mechanical)

Faculty of Mechanical Engineering  
Universiti Teknologi Malaysia

MARCH 2006

## ACKNOWLEDGEMENT

The completion of this work was possible with the support of many individuals. Although it is not possible to list all of them here, I would like to mention a few who deserve my deepest appreciation.

I wish to express my sincere gratitude to my thesis supervisors, Assoc Prof Dr. Tholudin and Dr. Jamaluddin, for their guidance, support and advice throughout my research.

I would also like to thank my parents, sisters and brothers for their love and support to pursue my graduate studies.

I am very grateful to Mr. Muthu and family for their caring, support and encouragement throughout my studies. Their financial support really helps me to finish this study.

I must thank my fiancée, Miss Letchumy Praba for her invaluable support and encouragement. She has always been with me during good and bad times.

## ABSTRACT

Three dimensional low Mach number film cooling of turbine blade have been conducted using computational fluid dynamics (CFD) software FLUENT. Strong anisotropic of film cooling turbulence and flow complexities require capable turbulence model such as Reynolds Stress Model (RSM) or Large Eddy Simulation (LES) model to solve film cooling flow field. Film cooling with holes arrangement on blade leading edge, pressure and suction were tested in present study. The effects of film cooling parameters such as blowing ratio, surface curvature, injection angle, hole spacing, hole length, and plenum geometry have been investigated. The results presented in adiabatic film cooling effectiveness as well as plots of temperature and velocity contour. Present study reveals that blowing ratio, injection angles and coolant holes arrangements are significant parameters in film cooling process. Performances of film cooling highly depend on a combination of parameters. Present study represents the feasibility of CFD utilization as an innovative predictive tool in turbine blade film cooling design.

## ABSTRAK

Aliran penyejukan saput bilah turbin tiga dimensi dengan nombor Mach yang rendah di jalankan menggunakan perisian pergerakan bendalir berkomputer, FLUENT. Aliran gelora penyejukan saput yang tidak terarah dan struktur aliran yang kompleks memerlukan model aliran gelora yang berkebolehan seperti Reynolds Stress Model (RSM) atau Large Eddy Simulation (LES) untuk penyelesaian. Penyejukan saput dengan aturan lubang pada pinggir depan, permukaan cembung dan cekung bilah di kaji. Kesan parameter penyejukan saput seperti nisbah pancutan, kelengkungan permukaan, sudut pancutan, jeda lubang, panjang saluran bahan penyejuk, bentuk lubang dan geometri ruang pembekal penyejuk turut dikaji. Keputusan kajian dipersembahkan dalam bentuk kecekapan adiabatik penyejukan saput serta melalui plot kontor suhu dan halaju. Perbincangan keputusan adalah berdasarkan pengaruh parameter ini ke atas struktur aliran penyejukan saput. Kajian ini memdedahkan bahawa nisbah pancutan, sudut pancutan dan susunan lubang mempunyai kesan yang ketara keatas kecekapan penyejukan saput.

## TABLE OF CONTENTS

CHAPTER	TITLE	PAGE
	DECLARATION	ii
	ACKNOWLEDGEMENTS	iii
	ABSTRACT	iv
	ABSTRAK	v
	TABLE OF CONTENTS	vi
	LIST OF TABLES	x
	LIST OF FIGURES	xi
	LIST OF SYMBOLS	xxiv
	LIST OF APPENDIX	xxvi
<b>1</b>	<b>INTRODUCTION</b>	<b>1</b>
	1.1 Problem Statement	1
	1.2 Objective	3
	1.3 Scope of Research	3
	1.4 Outline of Thesis	4
<b>2</b>	<b>LITERATURE REVIEW</b>	<b>6</b>
	2.1 Film Cooling Theory and Fundamentals	6
	2.2 Computational Studies on Film Cooling	9
	2.3 Film Cooling Flow Structure	12
	2.3.1 Kidney Shaped Counter-Rotating Vortex Pair (CRVP)	13
	2.3.2 Horseshoe Vortices	14
	2.3.3 Vortices in Wake of Jet	15
	2.4 Parameter Affecting the Film Cooling	

	Flow Field	15
	2.4.1 Blowing Ratio	16
	2.4.2 Surface Curvature	17
	2.4.3 Jet Injection Angle.	17
	2.4.4 Free stream Turbulence Intensity	18
	2.4.5 Jets Spacing, Staggering and Hole Shape	19
	2.4.6 Coolant Hole Length and Plenum Geometry	21
2.5	Summary of Literature Review	21
<b>3</b>	<b>METHODOLOGY</b>	<b>23</b>
3.1	Turbine Blade Description	24
3.2	Governing Equations	27
3.3	Solution Technique	28
	3.3.1 Control Volume Approach	28
	3.3.2 Discretisation Schemes	29
	3.3.2.1 First Order Upwind Scheme	30
	3.3.2.2 Power Law Scheme	30
	3.3.2.3 Second Order Upwind and QUICK Scheme	31
3.4	Computational Meshes	32
	3.4.1 Mesh Generation	32
	3.4.2 Mesh Assessment	34
3.5	Turbulence Modeling	37
	3.5.1 Large Eddy Simulation (LES)	37
	3.5.2 Reynolds Averaged Navier-Stokes Equations (RANS)	39
3.6	Wall Treatment	41
3.7	Thermo physical Properties	43
	3.7.1 Flow Reynolds Number	43
3.8	Boundary Conditions	44
	3.8.1 Inlet Boundary	44
	3.8.2 Outlet Boundary	45

	3.8.3	Periodic Boundary	45
	3.8.4	Wall Boundary	45
	3.9	Solving Coupled Equations	46
	3.9.1	Relaxation Factors	47
	3.9.2	Time Step for LES simulation	47
	3.10	Convergence Tolerance Option	48
	3.10.1	Monitoring Mass Flow Rate	49
	3.10.2	Monitoring Wall Shear Stress	49
	3.11	Calculation of the Adiabatic Effectiveness	49
	3.12	User Defined Function (UDF)	50
<b>4</b>		<b>VALIDATION AND BENCHMARK</b>	
		<b>SOLUTION</b>	51
	4.1	Benchmark Solutions	52
	4.1.1	Computational Domain and Flow Parameters	51
	4.2	Mesh Refinement Study	55
	4.2.1	Flat Plat Simulation	55
	4.2.2	Leading Edge simulation	57
	4.3	Simulation Results	60
	4.3.1.	Flat Plat Film Cooling Flow Field	60
	4.3.2	Flat Plat Adiabatic Cooling Effectiveness Results	66
	4.3.3	Turbulence Models and Wall Functions Evaluation	68
	4.3.4	Leading Edge Film Cooling Flow Field	70
	4.3.5	Leading Edge Adiabatic Film Cooling Effectiveness	78
	4.3.6	Turbulence Models and Wall Functions Evaluation	81
	4.4	Comparison between k- $\epsilon$ Model and LES Model for Flat Plat	83

4.5	Conclusion Drawn From Benchmark Studies	87
<b>5</b>	<b>RESULTS AND DISCUSSION</b>	<b>88</b>
5.1	The Flow and Thermal Field	88
5.1.1	Leading Edge	89
5.1.2	Suction Surface	103
5.1.3	Pressure Surface	108
5.2	Evaluation of Turbulences Models	114
5.2.1	Leading Edge	115
5.2.2	Suction Surface	120
5.2.3	Pressure Surface	125
5.3	Validation of Numerical Results	132
5.4	Effects of Parameters	136
5.4.1	Blowing Ratio	136
5.4.2	Combustion Gaseous Turbulence Intensity	144
5.4.3	Effect of Geometrical Parameters	148
5.4.3.1	Leading Edge	148
5.4.3.2	Suction Surface	150
5.4.3.3	Pressure Surface	154
<b>6</b>	<b>CONCLUSIONS AND RECOMMENDATIONS</b>	<b>158</b>
6.1	Summary	158
6.1.1	Film Cooling Flow Field on Turbine Blade	158
6.1.2	Turbulence Model Evaluation	159
6.1.3	Effects of Film Cooling Parameters	159
6.2	Recommendations for Future Study	160
	<b>REFERENCES</b>	<b>161</b>
	<b>Appendix A</b>	<b>169</b>



## LIST OF TABLES

TABLE NO.	TITLE	PAGE
3.1 (a)	Coolant holes locations on blade surface	26
3.1 (b)	Values of flow and geometrical variables	26
3.2	Comparisons between first order upwind and QUICK Scheme	31
3.2	Boundary conditions value	41
3.4	Interpolation scheme utilized in present simulation	47
3.5	Convergence tolerance factors used in FLUENT simulations	48
4.1	Parameters corresponding to (Schmidt <i>et al.</i> , 1996)	54
4.2	Parameters corresponding (Cruse <i>et al.</i> , 1997)	55
5.1	Coolant holes configurations at blade leading edge	149

## LIST OF FIGURES

FIGURE NO.	TITLE	PAGE
1.1	General schematic of turbine blade film cooling and flow structures (Garg, V.K, 2002)	2
2.1	Turbine blade film cooling holes	6
2.2	Schematic of film cooling on turbine blade (Hass <i>et al.</i> , 1992)	6
2.3	Standard circular film cooling hole nomenclature (Immarigeon, A.A, 2003)	8
2.4	Jet in cross flow (Fric and Roshko, 1994)	12
2.5	Vortex filament interaction (Morton and Ibbetson, 1996)	13
2.6	Free stream turbulence intensity effects on film cooling (Mayhew <i>et al.</i> , 2004)	19
2.7	Hole configuration (Youn and Kim, 2003)	20
3.1	Cascade configurations	24
3.2(a)	Cooling hole location	25

3.2(b)	Holes location at leading edge	25
3.2(c)	Holes location at suction surface	25
3.2(d)	Holes location at pressure surface	25
3.3(a)	Mesher at blade leading edge with coolant supply and plenum with density 255,856 cells	34
3.3(b)	Blade surface and coolant hole interface	34
3.4(a)	Centreline adiabatic film cooling effectiveness for various grid densities at, $M=1$ , RSM model	36
3.4(b)	Lateral distribution of adiabatic effectiveness on cross stream plane at $M=1$ , RSM model	36
3.5	Subdivision of the Near-Wall Region	42
3.6	Boundary conditions on computational domain	44
4.1	Test section geometry and coordinate system (Schmidt <i>et al.</i> , 1996)	53
4.2	Computational domains corresponding (Schmidt <i>et al.</i> , 1996)	53
4.3	Experimental model of leading edge film cooling (Cruse <i>et al.</i> , 1997)	54
4.4	Computational domains corresponding (Cruse <i>et al.</i> , 1997)	54
4.5	Centreline effectiveness predictions with $k-\epsilon$ model and standard wall function for flat plate film cooling $M=0.5$	56

4.6(a),(b)	Lateral effectiveness predictions with $k-\varepsilon$ model and standard wall function for flat plat at cross-stream perpendicular plane, $M=0.5$	57
4.7	Centreline effectiveness predictions with $k-\varepsilon$ model and standard wall function for leading edge film cooling, $M=2.0$	58
4.8(a),(b)	Lateral adiabatic film cooling effectiveness with $k-\varepsilon$ model and standard wall function for leading edge, $M=2.0$	59
4.9	Computed velocity vectors on centerline plane, $Z=0$ within coolant supply hole with $k-\varepsilon$ model and standard wall function	60
4.10(a)	Computed velocity vectors in cross stream perpendicular at $x/D=2.0$ with $k-\varepsilon$ model and standard wall function, $M=1.0$	61
4.10(b)	Superimposed of velocity vector on temperature contour at $x/D=2$ , with model and standard wall function, $M=1.0$	61
4.10(c)	Computed pressure contour in cross stream perpendicular at $x/D=2.0$ with $k-\varepsilon$ model and standard wall function	62
4.10(d)	Computed pressure contour in cross stream perpendicular at $x/D=2.0$ and $x/D=6$ with $k-\varepsilon$ model and standard wall function, $M=1.0$	62
4.11(a)	Computed temperature contour on centerline plane ( $Z=0$ ), shows effect of blowing ratio on trajectory of coolant jet	63
4.11(b)	Computed temperature contour on test surface	63

4.11(c)	Computed turbulence intensity contours at centerline plane	64
4.12(a)	Computed velocity vectors at vicinity of coolant hole on centerline plan using standard wall function, $M=1.0$	65
4.12(b)	Turbulence intensity contour at vicinity of coolant hole, $M=1.0$	65
4.13(a)	Centreline adiabatic film cooling effectiveness, $k-\varepsilon$ model and standard wall function	66
4.13(b)	Centreline adiabatic film cooling effectiveness, $k-\varepsilon$ model and standard wall function	67
4.13(c)	Local lateral adiabatic cooling effectiveness $k-\varepsilon$ model and standard wall function	67
4.14(a)	Centreline adiabatic film cooling effectiveness with standard wall function, $M=1.0$	68
4.14(b)	Centreline adiabatic film cooling effectiveness with non equilibrium wall function, $M=1.0$	69
4.14(c)	Centreline adiabatic film cooling effectiveness with Enhanced wall treatment, $M=1.0$	68
4.14(d)	Centreline adiabatic film cooling effectiveness with RSM turbulence model, $M=1.0$	70
4.15	Velocity vectors plot on stagnation plane, RSM model with standard wall functions, $M=2.0$	71

4.16	Pressure contour plot on lateral planes, RSM model with standard wall functions, $M=2.0$	72
4.17	First holes and second holes coolant jets path lines plot, RSM model with standard wall function, $M=2.0$	73
4.18(a)	Velocity vectors plots on cross stream plane, $s/D=4.86$ RSM model with standard wall functions, $M=2.0$	73
4.18(b)	Velocity vectors plots on cross stream plane, $s/D=4.86$ and $s/D=9.98$ , RSM model with standard wall functions, $M=2.0$	74
4.19(a)	Temperature contour plots on lateral planes, RSM model with standard wall functions, $M=2.0$	74
4.19(b)	Temperature contour plot on leading surface, RSM model with standard wall functions, $M=2.0$	75
4.20	Turbulence intensity contour plots on lateral planes, RSM model with standard wall functions, $M=2.0$	76
4.21(a)	Velocity vectors plot on plane $s/D=4.86(s_2)$ , $M=2.0$	77
4.21(b)	Turbulence intensity contour plot on plane Z3, $M=2.0$	77
4.21(c)	Temperature contour plot on leading edge, $M=2.0$	78
4.22(a)	Laterally averaged adiabatic cooling effectiveness along stream direction, $k-\epsilon$ model with standard wall functions, $M=2.0$	79
4.22(b)	Adiabatic film cooling effectiveness at lateral planes, $s/D=1.24$ , $k-\epsilon$ model with standard wall functions, $M=2.0$	79

4.22(c)	Adiabatic film cooling effectiveness at lateral planes, s/D=4.86, k- $\epsilon$ model with standard wall functions, M=2.0	80
4.22(d)	Adiabatic film cooling effectiveness at lateral planes, s/D=9.98, k- $\epsilon$ model with standard wall functions, M=2.0	80
4.23(a)	Laterally averaged film cooling effectiveness on leading edge, M=2.0	81
4.23(b)	Laterally averaged film cooling effectiveness on leading edge, M=2.0	82
4.23(c)	Laterally averaged film cooling effectiveness on leading edge, M=2.0	82
4.23(d)	Laterally averaged film cooling effectiveness on leading edge, M=2.0	83
4.24(a)	Temperature contour on flat surface using k- $\epsilon$ and LES, M=1.0	84
4.24(b)	Computed velocity vectors at vicinity of coolant hole on centreline plan, LES, M=1.0	84
4.25 (a)	Flat plat local lateral adiabatic cooling effectiveness, X/D=3	85
4.25(b)	Flat plat local lateral adiabatic cooling effectiveness, X/D=10	86
4.26	Flat plat centerline adiabatic film cooling effectiveness, M=1.0	86
5.1	Temperature contour on leading edge surface, M=2.0,	

	$\beta=30^0$ , RSM turbulence model	89
5.2	Velocity vector plot at stagnation downstream of suction surface, $M=2.0$ , $\beta=30^0$ , RSM model	90
5.3	Temperature contour of coolant jets on cross stream planes, $M=2.0$ , $\beta=30^0$ , RSM model	91
5.4	Temperature contour of coolant jets on span wise cut cross planes, $M=2.0$ , $\beta=30^0$ , RSM model	92
5.5(a)	Temperature contour of blade on span wise cut cross planes, $M=2.0$ , $\beta=30^0$ , RSM model	92
5.5(b)	Temperature contour of cross stream plane at various blade location, $M=2.0$ , $\beta=30^0$ , RSM model	93
5.6(a)	Velocity vector of coolant jets at stagnation on cross stream plane, $M=2.0$ , $\beta=30^0$ , RSM model	96
5.6(b)	Velocity contour of coolant jets at stagnation on cross stream plane $M=2.0$ , $\beta=30^0$ , RSM model	96
5.6(c)	Pressure contour of coolant jet at stagnation on span wise cut cross planes, $M=2.0$ , $\beta=30^0$ , RSM model	97
5.7(a)	Velocity vector of coolant jets at downstream of the stagnation on the suction surface on cross stream plane, $M=2.0$ , $\beta=30^0$ , RSM model	97
5.7(b)	Velocity contour of coolant jets at downstream of the stagnation on the suction surface on cross stream plane, $M=2.0$ , $\beta=30^0$ , RSM model	98



5.7(c)	Pressure contour of coolant jets at downstream of the Stagnation on the suction surface on span wise cut cross plane, $M=2.0$ , $\beta=30^0$ , RSM model	98
5.8(a)	Pressure contour of coolant jets at downstream of the Stagnation on the pressure surface on cross stream plane, $M=2.0$ , $\beta=30^0$ , RSM model	99
5.8(b)	Velocity contour of coolant jets at downstream of the stagnation on the pressure surface on cross stream plane, $M=2.0$ , $\beta=30^0$ , RSM model	99
5.8(c)	Velocity vector of coolant jets at downstream of the stagnation on the pressure surface on span wise cut cross plane, $M=2.0$ , $\beta=30^0$ , RSM model	100
5.9(a)	Interaction between coolant jets at stagnation region with jets at stagnation downstream of suction surface	101
5.9(b)	Interaction between coolant jets at stagnation region with jets at stagnation downstream of pressure surface	102
5.9(c)	Interaction between coolant jets at stagnation downstream of suction surface with jets at stagnation downstream of pressure surface	102
5.10	Temperature contour on blade suction surface, $M=1.0$ , RSM turbulence model	103
5.11	Temperature contour of coolant jets centerline plane on suction surface, $M=1.0$ , RSM turbulence model	104

5.12	Temperature contour of coolant jets at cross stream planes on suction surface, $M=1.0$ , RSM turbulence model	105
5.13	Velocity vectors of coolant jets at cross stream planes on suction surface, $M=1.0$ , RSM turbulence model	105
5.14	Superimposed of temperature contour and velocity vectors at cross stream planes on suction surface, $M=1.0$ , RSM turbulence model	106
5.15	Turbulence intensity contour on suction surface, $M=1.0$ , RSM turbulence model	107
5.16	Temperature contour on blade pressure surface, $M=1.5$ , RSM turbulence model	109
5.17	Temperature contour of coolant jets centerline plane on pressure surface, $M=1.5$ , RSM turbulence model	109
5.18	Temperature contour of coolant jets at cross stream planes on pressure surface, $M=1.5$ , RSM turbulence model	111
5.19	Velocity vectors of coolant jets at cross stream planes on pressure surface, $M=1.5$ , RSM turbulence model	111
5.20	Superimposed of temperature contour and velocity vectors at cross stream planes on pressure surface, $M=1.5$ , RSM turbulence model	112
5.21	Turbulence intensity contour on pressure surface, $M=1.5$ , RSM turbulence model	113
5.22	Schematic representation of LES and RANS approach, presented in spectral space (Felten, 2003)	114

5.23(a)	Temperature contour on leading edge surface, $M=2.0$ , $\beta=30^0$	115
5.23(b)	Temperature contour at lateral span plane, $Z/D=3$ , $M=2.0$ ,	115
5.24	Adiabatic film cooling effectiveness in lateral direction of blade leading edge, $M=2.0$ , $\beta=30^0$	118
5.25	Adiabatic film cooling effectiveness in mainstream direction in lateral plane of blade leading edge, $M=2.0$ , $\beta=30^0$	120
5.26(a)	Temperature contour on suction surface, $M=1.0$	121
5.26(b)	Temperature contour of coolant jets centerline lateral plane of suction surface, $Z/D=2$ , $M=1.0$	121
5.26(c)	Temperature contour at cross stream planes on suction surface, $M=1.0$	122
5.27	Adiabatic film cooling effectiveness in lateral direction at cross stream planes, $M=1.0$	124
5.28	Adiabatic film cooling effectiveness in stream direction of suction surface, $M=1.0$	125
5.29(a)	Temperature contour on pressure surface, $M=1.5$	126
5.29(b)	Temperature contour of coolant jets centerline lateral plane of pressure surface, $Z/D=2$ , $M=1.5$	126
5.30	Temperature contour at cross stream planes on pressure surface, $M=1.5$	127
5.31	Superimposed of temperature contour and velocity vectors at cross stream planes on pressure surface, $M=1.5$	128

5.32	Adiabatic film cooling effectiveness in lateral direction at cross stream planes, $M=1.5$	130
5.33	Adiabatic film cooling effectiveness in stream direction of pressure surface, $M=1.5$	131
5.34	Stream wise adiabatic film cooling effectiveness comparisons on suction surface	133
5.35	Laterally averaged adiabatic film cooling effectiveness comparisons on suction surface	134
5.36	Stream wise adiabatic film cooling effectiveness comparisons on pressure surface	134
5.37	Laterally averaged adiabatic film cooling effectiveness comparisons on pressure surface	137
5.38(a)	Temperature contour on suction surface, LES model	138
5.38(b)	Temperature contour on suction surface at lateral plane, $Z/D=2$ , LES model	138
5.38(c)	Stream wise adiabatic film cooling effectiveness on suction surface at lateral plane, $Z/D=2$ , LES model	139
5.38(d)	Laterally averaged adiabatic film cooling effectiveness on suction surface, LES model	139
5.39(a)	Temperature contour on pressure surface, LES model	141
5.39(b)	Temperature contour on pressure surface at lateral plane, $Z/D=3$ , LES model	141

5.39(c)	Velocity vectors plot at cross stream of pressure surface at $X/D=2$ , LES model	142
5.39(d)	Velocity vectors plot at cross stream of pressure surface at $X/D=4$ , LES model	142
5.39(e)	Velocity vectors plot at cross stream of pressure surface at $X/D=8$ , LES model	142
5.39(f)	Stream wise adiabatic film cooling effectiveness on pressure surface at lateral plane, $Z/D=3$ , LES model	143
5.39(g)	Laterally averaged adiabatic film cooling effectiveness on pressure surface, LES model	143
5.40(a)	Stream wise adiabatic film cooling effectiveness on leading edge at lateral plane, $Z/D=3$ , $M=2.0$ LES model	145
5.40(b)	Laterally averaged adiabatic film cooling effectiveness on leading edge, $M=2.0$ , LES model	146
5.41(a)	Stream wise adiabatic film cooling effectiveness of pressure surface at lateral plane, $Z/D=3$ , $M=1.5$ , LES model	146
5.41(b)	Laterally averaged adiabatic film cooling effectiveness on pressure surface, $M=1.5$ , LES model	147
5.42	Stream wise adiabatic film cooling effectiveness of suction surface at lateral plane, $Z/D=2$ , $M=1.0$ , LES model	147
5.43	Laterally averaged adiabatic film cooling effectiveness of blade leading edge, $M=2.0$ , LES model	149
5.44(a)	Stream wise adiabatic film cooling effectiveness of	

	suction surface at lateral plane, $Z/D=2$ , $M=0.5$ , LES model	151
5.44(b)	Stream wise adiabatic film cooling effectiveness of suction surface at lateral plane, $Z/D=2$ , $M=1.0$ , LES model	151
5.45(a)	Stream wise adiabatic film cooling effectiveness of suction surface at lateral plane, $Z/D=2$ , $M=0.5$ , LES model	152
5.45(b)	Laterally averaged adiabatic film cooling effectiveness of suction surface, $M=0.5$ , LES model	152
5.45(c)	Stream wise adiabatic film cooling effectiveness of suction surface at lateral plane, $Z/D=2$ , $M=1.0$ , LES model	153
5.45(d)	Laterally averaged adiabatic film cooling effectiveness of suction surface, $M=1.0$ , LES model	153
5.46(a)	Stream wise adiabatic film cooling effectiveness of pressure surface at lateral plane, $Z/D=3$ , $M=1.0$ , LES model	155
5.46(b)	Stream wise adiabatic film cooling effectiveness of pressure surface at lateral plane, $Z/D=2$ , $M=1.5$ LES model	155
5.47(a)	Stream wise adiabatic film cooling effectiveness of pressure surface at lateral plane, $Z/D=3$ , LES model	156
5.47(b)	Laterally averaged adiabatic film cooling effectiveness of pressure surface, LES model	156
5.47(c)	Stream wise adiabatic film cooling effectiveness of pressure surface at lateral plane, $Z/D=3$ , LES model	157
5.47(d)	Laterally averaged adiabatic film cooling effectiveness of pressure surface, LES model	157

## LIST OF SYMBOLS

$b$	-	Constant in the turbulence transport equations
$C_p$	-	Specific heat at constant pressure, (kJ/kg.K)
$C_\mu$	-	Empirical constant or variable in the turbulence equations
$D$	-	Coolant Hole Diameter, (m)
$DR$	-	Density ratio, ( $DR=\rho_j/\rho_\infty$ )
$E$	-	Total Energy, (kJ)
$f$	-	Mixture fraction
$G_k, G_b$	-	Generations terms in the turbulence transport equations
$h$	-	Local heat transfer coefficient, ( $W/m^2 \cdot K$ )
$J$	-	Mass flux, Diffusion Flux ( $kg/m^2 \cdot s$ )
$K$	-	Thermal conductivity, ( $W/m \cdot K$ )
$k$	-	Turbulent kinetic energy, ( $m^2/s^2$ )
$k$	-	Mass Transfer Coefficient
$L$	-	Length of coolant hole, (m)
$M$	-	Blowing ratio, ( $\rho_j U_j / \rho_\infty U_\infty$ )
$m$	-	Mass (kg)
$P$	-	Pressure, ( $N/m^2$ ); also refers to first element of the wall
$p$	-	Spanwise distance/pitch between coolant holes centerline (m)
$q''$	-	Local heat flux at the wall, ( $W/m^2$ )
$Re$	-	Reynolds number, ( $\rho U D / \mu$ )
$S$	-	Modulus of the mean rate of strain tensor in the turbulence transport equations
$S_\epsilon, S_k$	-	Source term in the turbulence transport equations
$S_{ij}$	-	Rate of strain tensor in the Reynolds stress tensor
$T$	-	Temperature, (K)
$T_{aw}$	-	Adiabatic wall temperature, (K)

Ti	-	Turbulence Intensity
U	-	Averaged velocity components, (m/s)
$\overline{u'_i u'_j}$	-	Reynolds stress tensor
$u_\tau$	-	Frictional velocity, $(\sqrt{\frac{\tau_w}{\rho_w}})$
x	-	Streamwise distance measured from coolant hole center, (m)
y	-	Vertical distance measured blade surface, (m)
$y^+$	-	Non dimensional wall distance, $(\sqrt{\frac{\rho u_\tau y_p}{\mu}})$
$y_p$	-	Height of the first node P off the wall, (m)
z	-	Lateral distance /span wise of the blade (m)
$\alpha$	-	Injection / inclination angle of coolant jets
$\alpha_k, \alpha_\varepsilon$	-	Inverse effective Prandtl numbers for k and $\varepsilon$ in the turbulence transport equations
$\beta$	-	Orientation angle of coolant jets.
$\delta_{ij}$	-	Kronecker delta,
$\varepsilon$	-	Dissipation rate of turbulent kinetic energy, (m <sup>2</sup> /s <sup>3</sup> )
$\eta$	-	Local adiabatic film cooling effectiveness, $(\frac{T_{aw} - T_\infty}{T_j - T_\infty})$
$\overline{\eta}$	-	Spanwise averaged film cooling effectiveness, $(\frac{\overline{T}_{aw} - T_\infty}{T_j - T_\infty})$
$\mu$	-	Laminar dynamic viscosity, (kg/m.s)
$\mu_T$	-	Turbulent dynamic viscosity (kg/m.s)
$\nu$	-	Laminar kinematic viscosity, (s/m <sup>2</sup> )
$\rho$	-	Density, (kg/m <sup>3</sup> )
$\sigma_k, \sigma_\varepsilon$	-	Turbulent Prandtl numbers for k and $\varepsilon$ in the turbulence transport equations
$\tau$	-	Shear stress, (N/m <sup>2</sup> )



## CHAPTER 1

### INTRODUCTION

#### 1.1 Problem Statement

The needs of protection of a surface due to extreme thermal condition by means of a fluid film were applied in many applications. Harsh and extreme thermal environment such as inside combustion chamber and turbine blade can lead to failure of their surface walls. The continuous improvement in the performance of gas turbine engine necessitates a continuous increase in the turbine inlet temperature. The efficiency and power output of gas turbine engine increase with increment in turbine inlet temperature. It is estimated that for every 100 °F increase in this temperature, the power output increases by about 10% and the efficiency increases by about 1.5% Berhe and Patankar (1998).

Since the inlet temperature of present generation gas turbines are much higher than the melting temperature of the available alloys used to make turbine blades. Hence cooling of the turbine blades is a critical issue in gas turbine engine technology. A suitable cooling mechanism is needed in term to reduce the resulting high thermal stresses and to prolong the life of turbine blade under this extreme condition. Currently, turbine blades are cooled by a combination of internal and external cooling mechanism. Convection and impingement cooling are the methods used to cool the turbine blade internally.

Film cooling is most common cooling mechanism for external surface of turbine blades. Film cooling wherein cooler air from the compressor is bled thru cavities of connecting shaft and injected near the blade surface through holes or slots to provide a layer of cool fluid between the hot gaseous and the blade surface. The

objective of film cooling is to provide a blanket of cold film, which behaves as an insulation layer on blade surface or as a heat sink.

Film cooling on turbine blade is controlled by many variables that contribute significantly on cooling effectiveness and local heat transfer coefficient over blade surface. Figure 1.1 depicted the turbine blade film cooling and its flow structures. Film cooling mainly affected by the blowing ratio, surfaces curvature, the mainstream turbulence intensity, the holes injection and compound angle, the holes spacing and the hole geometry. Recent studies also highlighted the importance of coolant supply hole and plenum geometry film cooling application. Numbers of the film cooling research of the past 30 years has been conducted especially on flat plat. Goldstein (1971), Simoneau and Simon (1993) and Bunker R.S (2005) provided intensive reviews on film cooling research. Although many important explanations have been obtained from these studies such as the qualitative understanding of the effects of a number of film cooling variables the quantitative applicability of these explanations to cooling of actual turbine blades is much less known.

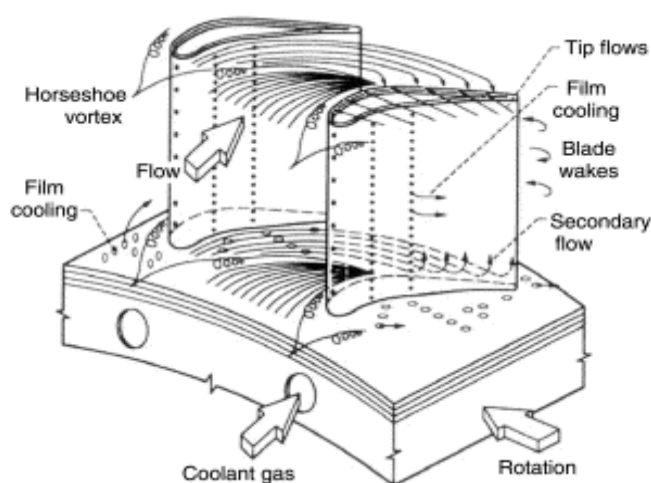


**Figure 1.1** General schematic of turbine blade film cooling and flow structures (Garg, V. K., 2002)

In film cooling application, especially on turbine vane and blade there are certain requirements must be considered. First, the coolant quantity should be the minimum possible. This is due to excessive coolant gases into the mainstream undercuts the production of useful power; this is because the coolant air that is taken from compression would go to produce real power. Moreover increased coolant

quantity will require more force to delivery it. Large quantity of coolant will interfere with the normal functioning of combustion gaseous and will reduce the gas turbine efficiency. Second, jet penetration into mainstream should be minimised. If jet penetration into mainstream is high, the coolant gases are lost into the mainstream instead of protecting the blade surfaces. Third, a good lateral spread of the coolant gases is important in order to provide uniform coolant coverage over the blade. Finally, the disruption to the blade aerodynamics must be minimum.

Film cooling studies on turbine by experimental test are very expansive and time consuming. Computational method in other hand gained popularity as alternative tool in current year. Computational fluid dynamic (CFD) can be a good and affordable tool when experimental test is impossible. Furthermore increase of storage capacity and computation speed may able to simulate complex flow problem with high accuracy and less cost compare to experimental test. This study proposes to investigate the turbine blade film cooling by computational method. Through computational fluid dynamic (CFD) the behaviour of turbine blade film cooling and its affecting parameters will be investigated. It is believed this work will provide a good contribution in understanding turbine blade film cooling.

## **1.2 Objective**

The goal of this study is to use numerical method to investigate the turbine blade film cooling effectiveness and its parameters.

## **1.3 Scope of Research**

In this study an investigation has been conducted to determine the effects of several film cooling parameters on cooling performance using commercial computational fluid dynamic (CFD) software, FLUENT. The blowing ratio, surface curvature, free stream turbulence intensity, coolant injection angle, compound angle

and holes spacing were investigated. The computational domain consists of main flow region, coolant hole and supply plenum placed at blade leading edge, suction and pressure surface. The main scope of this study directed as follows:

- 1) Benchmark studies and validation of computational aspects in film cooling application.
- 2) Investigate the ability of the computational model to accurately predict the film cooling application.
- 3) Simulate low Mach number three-dimensional turbine blade film cooling using anisotropic turbulence model.
- 4) Discuss and analyse effect of the film cooling parameters using computational data.

## **1.4 Outline of Thesis**

Chapter 2 of this thesis provide a literature reviews on film cooling research. This chapter start with brief review on film cooling theory and fundamentals and followed by reviews on computational studies on film cooling. Film cooling flow structures discussed in following section and then various film cooling parameters effects were discussed.

Research methodology been discussed in Chapter 3. Various computation aspects such as computation model, grid generation, governing equations, and turbulences models explained. FLUENT CFD components also reviewed in this chapter. In Chapter 4, results of validation and benchmark solution of flat plat film cooling and cylindrical leading edge film cooling presented and discussed. Grid independence and turbulences models been assessed to attain the yardstick for present simulation.

In Chapter 5 results and discussions on turbine blade film cooling are presented. Anisotropic turbulences models, RSM and LES utilised to conduct the simulation and both models were compared accordingly. Blade leading edge, suction and pressure surface film cooling investigated using temperature and velocity plots.

Film cooling adiabatic effectiveness calculated at stream direction and blade spans. Parametric variations on blade film cooling also presented in this chapter. The conclusion and recommendations for future work presented in Chapter 6.